Research Article

Cancer Immunology Research

Immunosurveillance and Immunoediting of Breast Cancer via Class I MHC Receptors

Megan M. Tu[1], Mir Munir A. Rahim[2], Céline Sayed[1], Ahmad Bakur Mahmoud[1,3], and Andrew P. Makrigiannis[1,2]

Abstract

Ly49 receptors, which recognize "self" class I major histocompatibility complex (MHC-I) molecules, enable natural killer (NK) cells to detect loss of MHC-I expression on transformed and virally infected cells. The impact of NK cell–mediated MHC-I surveillance on immunoediting of breast cancer is still not fully understood. This work assesses the impact of Ly49 receptors on tumor development in terms of cancer control and in driving immune-evading cancer mutations. Genetically modified Ly49-deficient mice and those lacking NK cells through antibody depletion were less able to control E0771-derived mammary tumors in an MHC-I–dependent fashion. Similarly, Ly49-deficient MMTV-PyVT–transgenic mice developed spontaneous mammary tumors faster than Ly49-sufficient MMTV-PyVT mice. Fewer $CD69^+$ and granzyme B^+ NK cells were detected among the tumor-infiltrating lymphocytes in Ly49-deficient than in Ly49-sufficient MMTV-PyVT mice. Furthermore, tumors from Ly49-deficient mice displayed reduced MHC-I expression, suggesting that tumors growing in these mice lacked an Ly49-derived pressure to maintain MHC-I expression. These same MHC-I-low tumors from Ly49-deficient mice were unable to flourish when transferred to Ly49-sufficient hosts, confirming that this tumor mutation was in response to an Ly49-deficient environment. This work demonstrates a role for Ly49 receptors in the control of mammary cancer, and provides evidence to support a model of tumor immunoediting, in which selective pressures from the immune system drive immune-evasive cancer mutations. *Cancer Immunol Res; 5(11); 1016–28. ©2017 AACR.*

Introduction

Breast cancer is the leading cause of cancer-related deaths among women globally (1). Although detection and treatment of the primary tumors have yielded many successes, conventional therapies such as surgery, chemotherapy, and radiation do not address the risk of relapse and metastatic disease. Moreover, tumors are heterogeneous (2), and some of these tumor subpopulations are highly propagative and resistant to radiation (3–5). For these reasons, we are interested in exploring avenues of treatment that involve augmenting the immune system's response.

In performing cancer immunosurveillance, the host immune system exerts pressure on a developing tumor, often eradicating cancerous cells before a tumor is established. However, this same immune pressure is believed to shape tumor development and select for mutations creating an immune-evasive cancer. This cancer-immune interaction proceeds in three phases, known as the "three Es" of cancer immunoediting. First, the immune system is able to eliminate many of the tumor cells. Next, the immune system enters equilibrium with those cancerous cells (6). Finally, the cancer cells develop enough resistance that they can escape the immune system, leading to a failure of immune-mediated cancer control.

Immune-targeting clinical interventions seek to break the bleak pattern described by the three Es, allowing for control of a tumor by the immune system. Adaptive immunity, and particularly the presence of tumor-infiltrating $CD8^+$ T cells, is crucial in the control of tumor cells and preventing overall cancer progression (7). For this reason, current immune therapies target these adaptive immune cells in an attempt to enhance their activity or longevity. The success of immune checkpoint inhibitors such as anti–CTLA-4 and anti–PD-1/–PD-L1 in the clinic emphasizes the efficacy of immune-based cancer therapy.

However, adaptive immunity is only one arm of the immune system, and there is mounting evidence for innate immune cells' involvement in cancer immunosurveillance. In particular, natural killer (NK) cells are involved in antitumor immunity, and the therapeutic potential of this population against cancer warrants study. In humans, NK cells comprise 10% to 15% of the lymphocytes in the peripheral blood. In mice, NK cells can control various tumor cell lines, spontaneously arising tumors, and tumors induced by chemical carcinogens (8, 9). In humans, studies that correlate disease with NK-cell absence or dysfunction show the value of NK cells. Lessened NK cell–mediated cytotoxicity is associated with increased risk of cancer development (10).

[1]Department of Biochemistry, Microbiology, and Immunology, University of Ottawa, Ottawa, Canada. [2]Department of Microbiology and Immunology, Dalhousie University, Halifax, Canada. [3]College of Applied Medical Sciences, Taibah University, Madinah Munawwarah, Saudi Arabia.

Note: Supplementary data for this article are available at Cancer Immunology Research Online (http://cancerimmunolres.aacrjournals.org/).

Corresponding Author: Andrew P. Makrigiannis, Dalhousie University, 5850 College St., Sir Charles Tupper Medical Building, room 7-C1, Halifax B3H 4H7, Canada. Phone: 902-494-2736; Fax: 902-494-5125; E-mail: amakrigiannis@dal.ca

doi: 10.1158/2326-6066.CIR-17-0056

As for T cells, NK-cell infiltration into tumors is prognostic of improved survival (11–13), even though NK-cell numbers and percentages remain low compared with those of other lymphocytes (14, 15).

The mouse lectin-like Ly49 family of receptors controls the reactivity of NK cells. Like their human homologues, the killer-cell immunoglobulin-like receptors (KIR), Ly49 receptors function by recognizing class I major histocompatibility complex (MHC-I) molecules on potential target cells. NK-cell activation is dependent on a balance of activating and inhibitory signals, with the dominant signal determining the response. Because MHC-I expression transmits an inhibitory signal to the NK cell through its Ly49 receptors, these NK cells are able to detect aberrant loss of MHC-I expression through a lack of an inhibitory signal; this phenomenon is known as "missing-self" recognition (16). NK cells are then able to elicit direct cytotoxicity through the production of perforin and granzymes, as well as recruitment of other immune cells through the release of pro-inflammatory cytokines. In addition to missing-self recognition, NK cells also recognize stress markers exhibited on the surface of aberrant cells, such as tumors or virally infected cells. These stress ligands are recognized by activating receptors on NK cells, which in turn induce NK activation (17).

Using mice deficient in the Ly49 family receptors, NKC^{KD} mice, we have previously shown that NK cells control leukemia and lymphoma (18). NKC^{KD} mice exhibit silenced Ly49 expression on approximately 80% of NK cells. In addition, expression of NKG2, CD94, and KLRI receptors—encoded by genes in the natural killer gene complex (NKC)—are downregulated on NK cells (19). Numbers of NK cells and expression of cell surface markers other than NKC are normal. Thus, these mice provide a suitable model to study the role of Ly49 receptors in cancer immunosurveillance, as we have shown earlier in Eμ-myc transgenic mice which develop B cell lymphoma (18, 19). However, hematologic cancers are not as immunologically challenging as a solid tumor, and the degree to which Ly49 receptors contribute to the control of solid malignancies remains unclear. A role for innate immune cells, which include NK and NKT cells, has been demonstrated in immune surveillance of methylcholanthrene (MCA)-induced sarcoma in mice (20, 21). Expansion of granzyme B-expressing innate lymphoid cell and innate-like T-cell populations, distinct from conventional NK and NKT cells, have been shown in oncogene-induced mammary tumors from MMTV-PyVT transgenic mice (22). Here, we show a role for NK cells and their Ly49 receptors in controlling breast cancer. We studied breast cancer because of its lethality and heterogeneity (23). The five molecular subtypes of breast cancer—luminal A, luminal B, ERBB2, basal, and normal-like—each exhibiting distinct gene expression patterns and different survival outcomes (24). Each could be treated with an immune-targeted approach. Here, we provide evidence for the role of NK cells and their Ly49 family receptors in control of pre-established tumor cells and developing tumors through a transgenic oncogene mouse model. Additionally, we show evidence for selective tumor immunoediting, wherein a different tumor surface-antigen expression signature is observed between mice possessing or lacking NK cells and the Ly49 receptors. We show that NK cells are able to infiltrate solid tumors, delay breast tumor development, and alter tumor protein expression.

Materials and Methods

Mice

C57BL/6 (B6) and MMTV-PyVT transgenic [strain: B6.FVB-Tg (MMTV-PyVT)634Mul/LellJ] mice were purchased from the Jackson Laboratory. MMTV-PyVT mice express the Polyoma virus middle T antigen under the control of the mouse mammary tumor virus promoter (25). $B6.Ly49^{129}$ and $B6.NKC^{KD}$ ($Klra15^{tm1.1Apma}$) mice have been previously described (19). Because of linkage disequilibrium, $B6.NKC^{KD}$ mice possess a 129-derived NKC. Therefore, the $B6.Ly49^{129}$ congenic mouse strain (26), which harbors a 129-derived NKC on the B6 background, serves as the genetically correct wild-type (WT) control. For brevity, $B6.NKC^{KD}$ and $B6.Ly49^{129}$ are referred to as NKC^{KD} and WT, respectively.

MMTV-PyVT mice were crossed with WT and NKC^{KD} mice to produce WT.MMTV-PyVT and NKC^{KD}.MMTV-PyVT mice, respectively. Genotyping for the MMTV-PyVT transgene was performed by PCR using primers: forward (5'to 3') GGA AGC AAG TAC TTC ACA AGG G and reverse (5' to 3') GGA AAG TCA CTA GGA GCA GGG to attain a PCR amplicon size of 556 bp. WT.MMTV-PyVT and NKC^{KD}.MMTV-PyVT were bred as homozygous and heterozygous mating pairs. Nonlittermate female WT.MMTV-PyVT and NKC^{KD}.MMTV-PyVT mice of similar age were housed separately or cohoused after weaning. Littermate versus nonlittermate (cohoused and noncohoused) mice were monitored and no differential effect on tumor incidence was observed within the same genotype.

All *in vivo* experiments were initiated in mice between 6 and 9 weeks of age. All mice were maintained in a specific-pathogen-free environment. Breeding and manipulations performed on animals were in accordance with and approved by the University of Ottawa Animal Ethics Committee (Ottawa, Ontario, Canada).

Purification of monoclonal antibody (mAb)

Anti-NK1.1 was produced in the lab from the hybridoma clone PK136 cultured in DMEM supplemented with 1 mmol/L sodium pyruvate, 0.1 mmol/L non-essential amino acids, 0.1 mmol/L β-mercaptoethanol, 100 U/mL penicillin, and 1 mg/ml streptomycin. Monoclonal Ab was purified from cell supernatants using Protein G sepharose chromatography (Exalpha Biologicals). Purified mAb was dialyzed in 1× PBS buffer (pH 7.4) and concentrated using an Amicon ultra-15 centrifugal filter unit with an ultracel-100 kDa membrane (EMD Millipore). The concentration was determined by SDS-PAGE and spectrophotometric measurement at 280 nm. For NK-cell depletion, 100 μL of 1 mg/ml anti-NK1.1 was injected intraperitoneally, at days −2, 0, 4, and every 3 days thereafter to maintain NK-cell depletion in these mice.

Cells, antibodies, and flow cytometry

The C57BL/6-derived breast cancer cell line E0771 was kindly provided by Dr. Ratna B. Ray (Saint Louis University), who originally obtained them from Dr. Rong Xiang (Scripps Institute).

MHC-I–deficient E0771 cells were generated by disrupting the $H\text{-}2K^b$ and $H\text{-}2D^b$ alleles of MHC-I using the CRISPR-Cas9 system as previously described (27). A 20-bp guide sequence (5′GCC CCG ACT CAG ACC CGC GC 3′) targeting DNA within the first exon of both H-2K and H-2D was selected using the CRISPR Design Tool (http://tools.genome-engineering.org) and checked using the UCSC Genome Browser for specificity and off-target hits. The single guide RNA (sgRNA) was ligated into the pSpCas9

(BB) (also known as pX330; Addgene plasmid ID: 42230) vector, and transformed into competent Stbl3 cells for storage. The sgRNA-containing vector was transfected into E0771 cells using Lipofectamine (Invitrogen), as per the manufacturer's instructions. E0771 cells lacking expression of both H-2K and H-2D were identified by antibody labeling and cell sorting. Cells were single-cell cloned, expanded, and checked once again for absence of both H-2K^b and H-2D^b expression.

Antibody staining was performed using anti-CD45 (30-F11; BioLegend), anti-CD49b (DX5; eBioscience), anti-NKp46 (29A1.4; eBioscience), anti-TCRβ (H57-597; BioLegend), anti-CD3 (145-2C11; eBioscience), anti-CD8 (53-6.7; BioLegend), anti-CD4 (GK1.5; eBioscience), live/dead (eBioscience), anti-Clr-b [4A6; kindly provided by Dr. Carlyle (University of Toronto)], anti-H-2K^b (AF6-88.5.5.3; eBioscience), anti–H-2D^b (KH95; BD Biosciences), anti-MULT1 (5D10; eBioscience), anti-pan RAE-1 (186107; R&D Systems), anti-CD69 (HI.2F3; eBioscience), anti-human granzyme B (GB12; Invitrogen), anti-FasL (MFL3; eBioscience), and anti-TRAIL (N2B2; eBioscience). Cells were acquired on a CyAN-ADP flow cytometer with Summit 4.3 software (Beckman Coulter) or LSR Fortessa (BD Biosciences) with FACSDiva software (BD Biosciences). Flow data were analyzed using Kaluza 1.2 software (Beckman Coulter).

Spontaneous mammary tumor model

Female MMTV-PyVT mice were monitored weekly for tumor development and scored as tumor positive if tumor width exceeded 3 mm and tumor exhibited progressive growth. Tumor size was determined using an electronic caliper (Marathon). Tumor growth rate (mm^2/day) was calculated based on the tumor area with respect to number of days since initial tumor development. Tumor-bearing mice were euthanized upon exhibiting progressively enlarged tumors exceeding 15 mm in width or length. The spleen was dissociated to attain a single-cell suspension. Tumors were removed and minced in 5 mL RPMI with 200 μg/mL collagenase D (Roche) and 20 μg/mL DNaseI (Roche), followed by incubation for 30 minutes at 37°C. The minced tumors were passed through a 100-μm cell strainer in order to obtain single-cell suspensions.

Splenocytes and tumor cells were incubated with Fc block (anti-CD16/CD32), then stained with antibodies as described above. Intracellular staining for granzyme B was performed using IC fixation and permeabilization reagents (eBioscience) following the manufacturer's instructions. Mean fluorescence intensity (MFI) for H-2K^b, H-2D^b, Clr-b, RAE-1, and MULT1 expression in the spleen and tumors of MMTV-PyVT mice was standardized to expression levels of splenocytes and mammary cells from the fat pads of WT control mice.

Mammary fat pad injections

Groups of female B6, WT (Ly49^{129} congenic), and NKC^{KD} mice were injected with 5×10^4 WT or CRISPR-mediated H-2K and H-2D knockout E0771 cells in the third left thoracic mammary fat pad. Some groups were depleted of NK cells using anti-NK1.1 mAb as described above. Mice were monitored for palpable tumors every 3 days postinjection. Tumor size was determined using an electronic caliper (Marathon) to measure length and width. Spleen and tumor cells were prepared for flow cytometry analysis as described above.

In vitro NK-cell cytotoxicity assay

Adherent lymphokine (IL2)-activated killer (ALAK) cells were grown in culture and used as effector cells in [^{51}Cr]-release cytotoxicity assays, as previously described (28).

In vitro stimulation of tumor infiltrating lymphocytes (TILs)

Lympholyte-M (Cedarlane) was used to purify lymphocytes from the single-cell tumor suspension. The isolated lymphocytes were incubated with YAC-1 cells at 1:1 ratio or with phorbol 12-myristate 13-acetate (PMA, 50 ng/mL) and ionomycin (1 μg/mL) in the presence of anti-CD107a mAb and brefeldin A (eBioscience) for 4 hours. Cells were stained for surface markers as described above, followed by intracellular staining for IFNγ using IC fixation and permeabilization reagents (eBioscience) following the manufacturer's instructions. NKp46$^+$TCRβ$^-$cells were analyzed for IFNγ by flow cytometry.

Quantitative real-time polymerase chain reaction (RT-qPCR)

Total RNA was isolated from WT mammary fat pads (control) and mammary tumor cells from MMTV-PyVT mice. Extraction of mRNA from cells was completed using RiboZol RNA Extraction Reagents (Amresco). Total RNA concentrations following extraction were calculated using a Nanodrop Spectrophotometer (ND-1000; Thermo Fisher Scientific). Quantitect Reverse Transcription Kit (Qiagen) was used to reverse transcribe 1 μg of RNA into cDNA. For qPCR analysis, 1/400 of the cDNA generated was used as a template and amplified with the KAPA SYBR FAST Universal qPCR Master Mix (Kapa Biosystems). RNA extraction, reverse transcription and qPCR amplification was performed as per the manufacturer's protocol. PrimerQuest Tool was used to generate primers that were validated before use. Reactions were performed and data collected using the Mastercycler Realplex^2 qPCR machine (Eppendorf). Samples were analyzed in duplicates and the average of the two values was used for further analysis. Data were analyzed using the ΔΔCT method to quantify gene expression (29). For this method, values obtained were first normalized to the values obtained for the amplification of 18S rRNA, and then normalized to WT mammary fat pads. These values were expressed for each respective gene. qPCR primer sequences: H-2K^b forward (5' to 3'): CAG ATA CCT GAA GAA CGG GAA C, H-2K^b reverse (5' to 3'): GCA CCT CAG GGT GAC TTT AT, H-2D^b forward (5' to 3'): CTC TTG GGA AGG AGC AGA ATT A, H-2D^b reverse (5' to 3'): AGC AAC GAT CAC CAT GTA AGA, 18S rRNA forward (5' to 3') CGCCGCTAGAGGTGAAATC, and 18S rRNA reverse (5' to 3') CCAGTCGGCATCGTTTATGG.

Statistical analysis

Statistical comparisons were performed on Kaplan–Meier plots depicting tumor onset using the log-rank test with Prism (GraphPad Software). For the remainder, statistical significance was determined by a two-tailed *t* test with cutoff *P* value of 0.05. *, $P < 0.05$; **, $P < 0.01$; ***, $P < 0.001$; and n.s., not significant.

Results

Absence of NK cells affects tumor growth and MHC-1 expression

Known NK cell targets include a variety of tumor cells of hematopoietic origins (16, 19, 30), and the medullary breast adenocarcinoma cell line E0771 (31, 32). Flow cytometry analysis revealed that E0771 cells express low to moderate levels of both

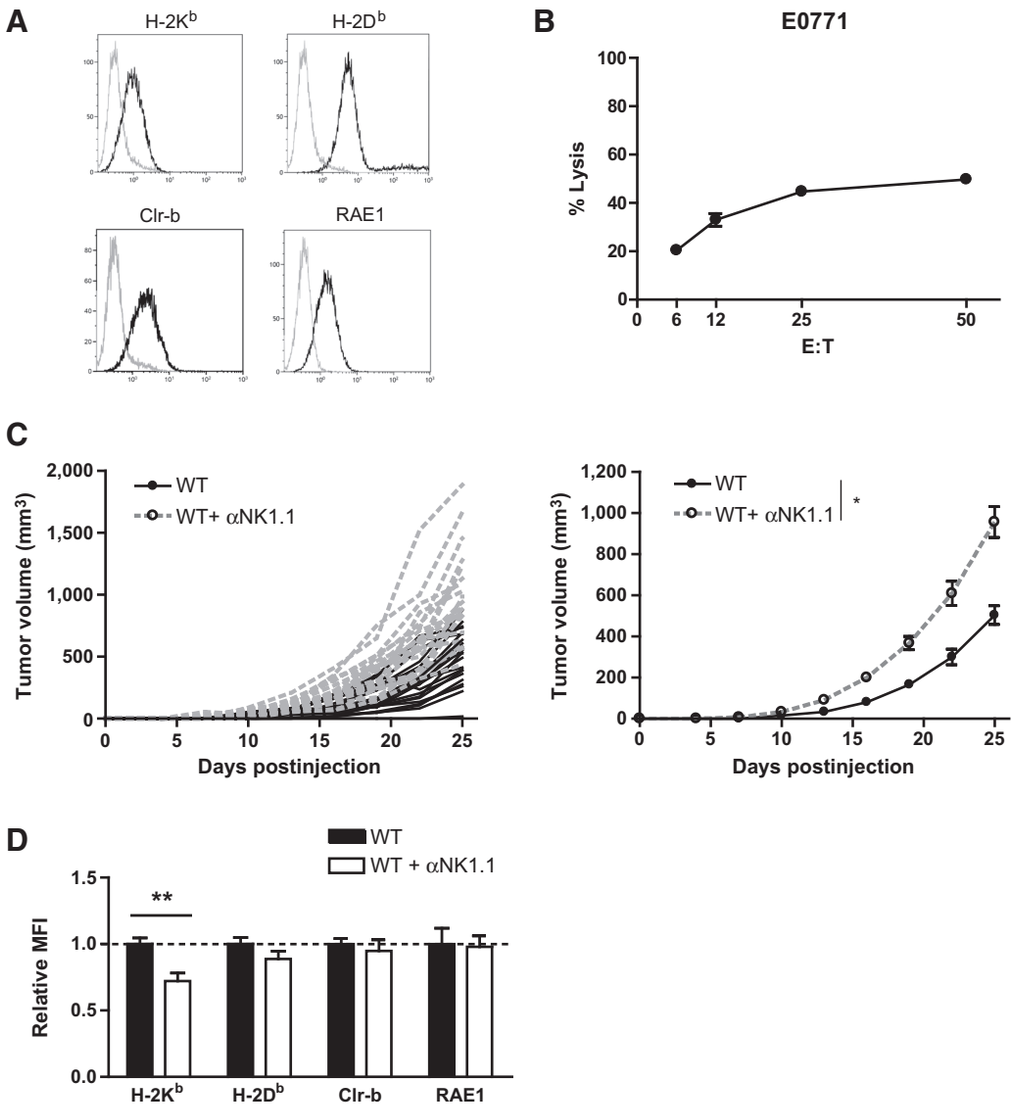

Figure 1.

Control of E0771 tumor cells is NK cell–dependent. **A,** Surface expression of H-2K^b, H-2D^b, Clr-b, and Rae1 on E0771 cells. **B,** Cytotoxicity assay showing killing of E0771 cells by B6-derived ALAKs. Data representative of four independent experiments. **C,** Formation of mammary tumors following injection of 5×10^4 E0771 cells into the mammary fat pad of groups of B6 ($n = 22$) and NK cell–depleted (αNK1.1) B6 mice ($n = 23$). Left, each line represents a single mouse. Right, mean ± SEM of tumor volume. Data pooled from six independent experiments. **D,** *Ex vivo* tumor analysis for surface expression of H-2K^b, H-2D^b, Clr-b, and Rae1 from B6 ($n = 18$) and NK cell–depleted B6 ($n = 19$) mice. Data pooled from five independent experiments.

MHC-I molecules, H-2K^b and H-2D^b, Clr-b—the ligand for the inhibitory NKR-P1B receptor—and RAE1, a ligand for the activating NKG2D receptor on NK cells (Fig. 1A). Using a chromium-51 release assay, we confirmed that adherent lymphokine-activated killer cells (ALAK) can recognize and kill E0771 cells, with increasing cytotoxicity at increasing effector to target ratios (Fig. 1B).

We asked whether NK cells can also control these mammary tumor cells *in vivo*. A total of 5×10^4 E0771 cells were injected into the fat pad of groups of B6 mice which were either treated with anti-NK1.1 to deplete NK cells, or left untreated. We observed that NK-cell depletion resulted in increased tumor growth compared with the untreated mice, supporting a role for NK cells in the control of mammary tumor development *in vivo*. The tumor progression in each mouse (Fig. 1C), as well as the mean tumor size over time (Fig. 1D), shows the NK cell–depleted group bearing larger tumors than the untreated group at comparable times. These tumors were analyzed following endpoint at day 25 for the presence of TILs. On average, 3% of the tumor-infiltrating immune cells were identified as NK cells in the undepleted mice, whereas less than 0.3% were found in the NK cell–depleted mice (Supplementary Fig. S1A). We observed no difference in the

percentage of $CD4^+$ or $CD8^+$ T cells in the NK cell–depleted or undepleted group (Supplementary Fig. S1B). The quantitative difference in NK-cell but not T-cell proportion between the two groups indicates that the accelerated tumor progression observed is a result of loss of NK cells.

Analysis of expression of antigens on the surface of the tumors revealed lower H-$2K^b$ expression on NK cell–depleted than undepleted mice, which is in line with the "missing-self" hypothesis (Fig. 1D). We analyzed tumor-infiltrating $CD4^+$ and $CD8^+$ T cells for IFNγ production; however, no differences were seen in the percentage of IFNγ expressing $CD4^+$ (Supplementary Fig. S1C) and $CD8^+$ (Supplementary Fig. S1D) between the undepleted and NK cell–depleted groups. As a result, we hypothesize that in the absence of NK cells, tumor cells with more H-$2K^b$ were recognized and killed by $CD8^+$ T cells, whereas those with less evaded detection and, therefore, comprised the bulk of the tumor at endpoint analysis. Analysis of the lungs for pulmonary metastases revealed no statistically significant difference in numbers of metastases, which were few (Supplementary Fig. S1E).

Defective recognition and control of tumors in mice lacking Ly49 receptors

Our previous work showed that mice lacking the Ly49 receptor family are defective in missing-self recognition of MHC-I–deficient tumors, but are otherwise normal in response to MHC-I expressing tumors (18). Therefore, to study the role of Ly49 receptors in the control of E0771 mammary tumors, we generated MHC-I–deficient mutants of E0771. Using CRISPR-Cas9 technology, we knocked-out both MHC-I molecules, H-$2K^b$ and H-$2D^b$ (Fig. 2A). WT E0771 cells were killed by WT and NKC^{KD}-derived ALAKs, as expected (Fig. 2B). However, killing of the MHC-I–deficient E0771 cells by NKC^{KD} ALAKs was much less than that of WT ALAKs at comparable effector to target ratios (Fig. 2C). Loss of MHC-I expression renders the E0771 target cells more susceptible to killing by WT NK cells. This was recapitulated *in vivo*, where MHC-I–deficient E0771 cells, but not WT, grew more rapidly in NKC^{KD} mice than in WT mice (Fig. 2D and E). Together, the data support a role for Ly49 receptors in the immunosurveillance of MHC-I–deficient mammary tumors by NK cells.

Ly49-dependent control and immunoediting of mammary tumors

Using MMTV-PyVT transgenic mice, we monitored the development of mammary tumors in mice on the WT or NKC^{KD} background to better understand the effect that silenced Ly49 expression had on breast cancer development. Female mice were monitored weekly for palpable tumors in any one of their ten mammary glands. Mice lacking expression of Ly49 receptors developed palpable tumors earlier on than their WT counterparts (Fig. 3A). The earliest tumor onset was detected in NKC^{KD} mice at day 62, compared with day 88 in WT mice. The first-arising tumor in each mouse was measured weekly and the tumor size was plotted relative to the age of the mouse (Fig. 3B). Tumors arising in NKC^{KD} mice grew faster than tumors arising in WT mice (Fig. 3C).

NKC^{KD} mice lack MHC-I–educated NK cells due to their loss of the Ly49 receptors. Although NK cells from mice with silenced Ly49 exhibit defective *in vitro* killing of tumor cells they would normally target (18–19), we are unable to rule out the contribution of tissue-resident type-1–like innate lymphoid cells (ILC1l) and type 1 innate-like T cells (ILTC1) in Ly49-mediated tumor immunosurveillance and immunoediting. We hypothesized that tumors in WT and NKC^{KD} mice would exhibit different properties as a result of their different microenvironment and immunoediting. The early- and end-stage tumors from WT and NKC^{KD} mice were analyzed for MHC-I expression and other ligands for activating and inhibitory receptors on NK cells—Clr-b, MULT1, and RAE1. The early-stage tumors act as a baseline for comparison throughout the cancer immunoediting stages of elimination, equilibrium, and escape (6). Early-stage tumors from WT and NKC^{KD} were comparable, with both exhibiting overall high H-$2K^b$ expression compared with the normal mammary fat pad and unaltered expression of other ligands (Fig. 4A and B). In comparison, the end-stage tumors of WT and NKC^{KD} differed. Tumors isolated from WT mice retained their higher levels of H-$2K^b$ (Fig. 4C), but tumors from NKC^{KD} exhibited low expression of H-$2K^b$ (Fig. 4D). The spleen was also analyzed to ensure that any differences seen were not the result of varied antibody staining, flow cytometry acquisition, or analysis. No change in the expression of any of the analyzed ligands was detected in the spleens from tumor-bearing compared with the healthy control mice (Fig. 4E and F).

We sought to determine the cause of this loss of H-$2K^b$ in end-stage tumors from NKC^{KD} mice. The flow cytometry-attained relative MFI values were compared with the qPCR-attained relative mRNA expression levels from the same tumor. If the mRNA is being transcribed and translated, even at lower rates than normal, we would expect to observe a plot where the overall slope would be close to 1 (linear correlation). In contrast, if mRNA was being transcribed normally, but encoded antigens were not presented at the cell surface due to defective translation or antigen processing, we would expect that the slope of the line would be greater than 1, as the relative qPCR values would exceed the relative MFI. The randomly dispersed pattern of the residual plot indicates a linear regression analysis is appropriate (Fig. 5). Overall, a linear correlation was observed for both H-$2K^b$ and H-$2D^b$ in WT and NKC^{KD}-derived tumors (Fig. 5). This suggested that the changes in MFI surface expression reflect changes in the mRNA levels within the cell.

Analysis of CD69 and granzyme B in tumor-infiltrating NK and T cells from tumors of MMTV-PyMT mice (Fig. 6A) show that there is more NK-cell activation in early-stage tumors from WT background compared with NKC^{KD} mice (Fig. 6B). This is not seen in the T- or NK-cell subsets from end-stage tumors (Fig. 6C). In contrast, splenic NK and T cells from tumor-bearing MMTV-PyVT are not activated (Supplementary Fig. S2). We hypothesize that MHC-I is upregulated and maintained on the tumors in WT mice in order to counteract activation of NK cells and possibly other immune cells that would express Ly49 receptors. In contrast, tumors that develop in the NKC^{KD} background do not need to maintain high MHC-I as these NK cells are hyporesponsive in response to missing self. Therefore, tumor surface MHC-I levels drop over time.

Analysis of the tumor-infiltrating NK cells and T cells in WT and NKC^{KD} mice in early versus late tumors revealed no difference in cell percentages (Supplementary Fig. S3A—S3D). IFNγ upregulates MHC-I expression (33). IFNγ is also required for T-cell–mediated tumor immunoediting (34). Therefore, we analyzed IFNγ production by tumor-infiltrating T cells in MMTV-PyVT transgenic mice on WT or NKC^{KD} backgrounds. Analysis of IFNγ production by $CD4^+$ and $CD8^+$ T cells revealed no differences (Supplementary Fig. S3E—S3H). Unfortunately, we were not able to detect NK cells for similar

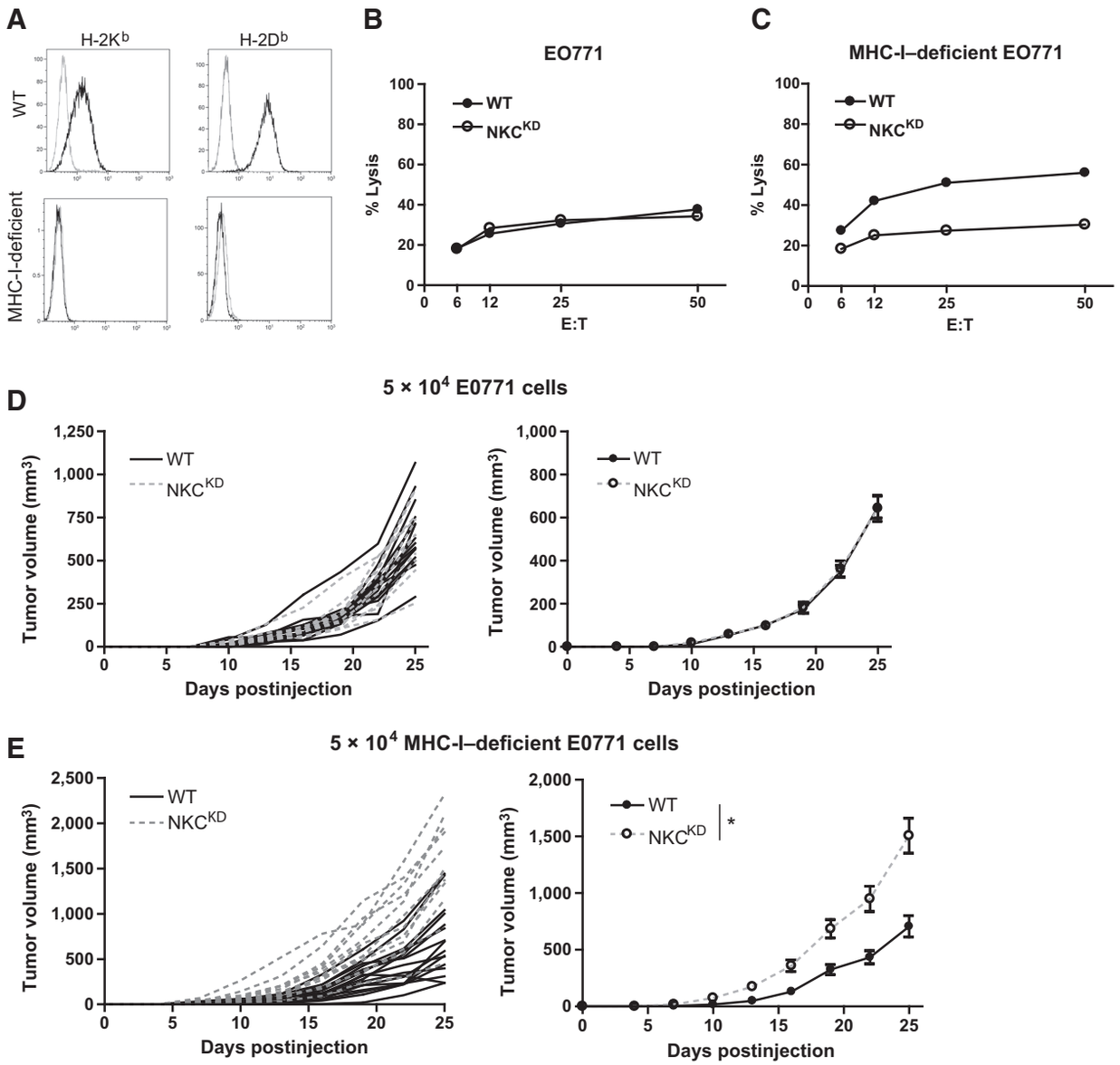

Figure 2.

Control of MHC-I–deficient E0771 is dependent on Ly49-mediated licensing. **A,** Surface expression of H-2K^b and H-2D^b on WT and CRISPR-Cas9–mediated H-2K and H-2D knockout (MHC-I–deficient) E0771 cells. **B,** Cytotoxicity assay showing killing of E0771 tumor cells by WT- and NKC^{KD} -derived ALAKs. Data representative of four independent experiments. **C,** Cytotoxicity assay showing killing of MHC-I–deficient E0771 tumor cells by WT- and NKC^{KD}-derived ALAKs. Data representative of three independent experiments. **D,** Formation of mammary tumors following injection of 5×10^4 E0771 cells into the mammary fat pad of groups of WT ($n = 15$) and NKC^{KD} ($n = 11$) mice. Left, each line represents a single mouse. Right, mean ± SEM. Data pooled from three independent experiments. **E,** Formation of mammary tumors following injection of 5×10^4 MHC-I–deficient E0771 cells into the mammary fat pad of groups of WT ($n = 16$) and NKC^{KD} ($n = 13$) mice. Left, each line represents a single mouse. Right, mean ± SEM. Data pooled from three independent experiments.

analysis following *in vitro* stimulation of TILs. Furthermore, FasL and TRAIL expression was not detected *ex vivo* on tumor-infiltrating NK cells in MMTV-PyVT mice (Supplementary Fig. S4). These observations suggest that the overall differences in tumor control are the result of hyporesponsive NK cells in NKC^{KD} mice, due to the silencing of the Ly49 receptors that support NK-cell recognition of aberrant cells.

MHC-I expression positively correlates with tumorigenesis of primary mammary tumors

Next, we determined whether the observed differences in H-2K^b in end-stage tumors from WT and NKC^{KD} affected their overall tumorigenicity. Tumors were resected from WT and NKC^{KD} mice, and single-cell tumor suspensions were injected into the mammary fat pads of groups of naïve WT mice. The WT-derived tumors

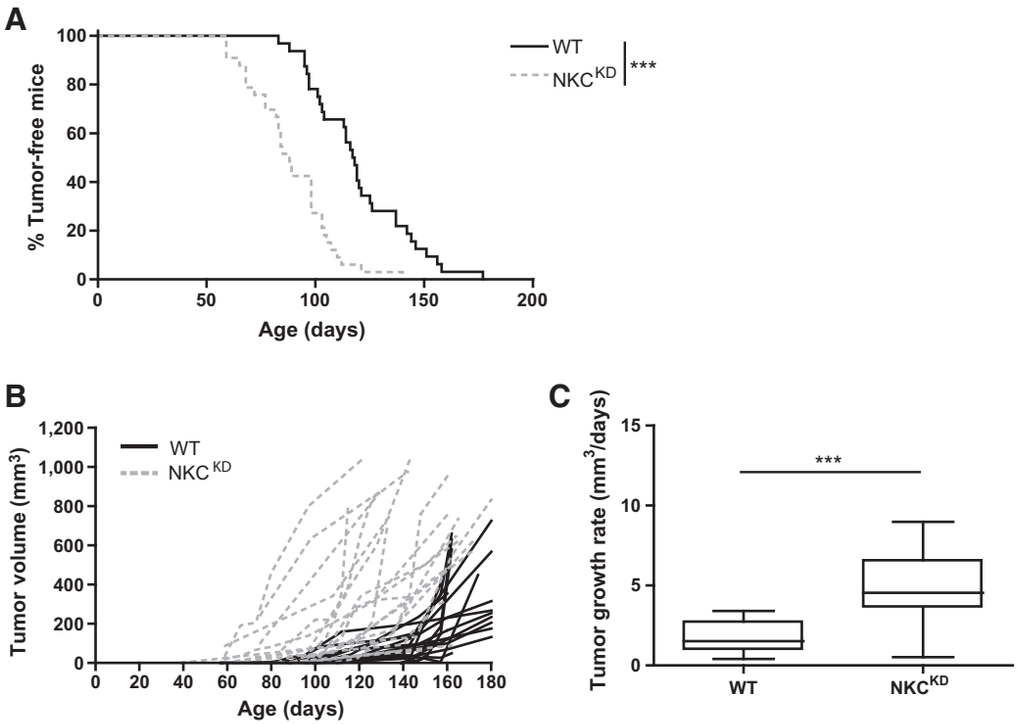

Figure 3.

NK cell–mediated control of mammary tumor development is Ly49 dependent. **A,** Mammary tumor development in NKC^{KD}.MMTV-$PyVT^{Tg}$ (NKC^{KD}; $n = 31$) and WT. MMTV-$PyVT^{Tg}$ (WT; $n = 31$) mice. **B,** Individual tumor growth measured weekly in MMTV-$PyVT^{Tg}$ mice on WT ($n = 20$) and NKC^{KD} ($n = 21$) background, with each line representing a single tumor. **C,** Tumor growth rate calculated from tumor size in **B**, with respect to time. Top and bottom limits of the box represent the 25th and 75th percentiles, with whiskers indicating minimum and maximum values. Each mouse represents an independent experiment.

with high MHC-I expression grew better following transplantation into WT naïve recipients than did NKC^{KD}-derived tumors with low MHC-I expression (Fig. 7A). To confirm that MHC-I levels were stable after transfer, we compared the MFI for MHC-I expression on day 0 and day 40 after transfer, and observed no change in either high or low H-$2K^b$ groups (Fig. 7B and C). Expression of H-$2D^b$, Clr-b, and RAE1 remained low and unchanged in both (Fig. 7B and C). We hypothesize that the development of MHC-I-low tumors in NKC^{KD} mice is in response to a hyporesponsive NK-cell environment, and that when those MHC-I-low tumors are transplanted into an environment with fully functional NK cells, they are recognized and killed (Fig. 7D).

Discussion

Innate immune cells, in particular NK cells, respond to various forms of malignancies. In addition to general immune defects such as reduced peripheral lymphocyte numbers and impaired IFNγ production, NK cell-specific alterations have also been identified in breast cancer patients (35). Here, we provide evidence from *in vivo* studies showing the importance of NK-cell receptors in breast cancer, supporting clinical observations and correlative assessments from human patient tumors. We show that breast tumor cells express markers that are recognized by both activating and inhibitory receptors on NK cells. In the absence of Ly49 expression, E0771-induced tumors grow more rapidly, and oncogene-driven spontaneous breast cancers appear earlier and grow faster than in mice with normal Ly49 expression. Upon analysis of the tumors that developed in a WT versus Ly49-deficient tumor microenvironment, we found differences in the expression of the MHC-I molecule, H-$2K^b$. Although early-stage tumors from both types of mice exhibit an upregulation of H-$2K^b$ expression, in late-stage tumors, H-$2K^b$ expression was lost in NKC^{KD} mice but not in WT mice. Fewer activated $CD69^+$ and granzyme B^+ NK cells were detected among TILs in the early-stage tumors from Ly49-deficient mice. Similarly, H-$2K^b$ is downregulated on E0771-induced tumors in the absence of NK cells. This evidence indicates tumor immunoediting. The similarities in early-stage tumors from WT and NKC^{KD} mice and the divergence between end-stage tumors (Fig. 4) suggests that tumors are molded over time by selective pressures exerted on them by the immune cells within the tumor microenvironment.

In the absence of a selective pressure via MHC-I receptors (Ly49), the tumors have evolved lower surface MHC-I expression, as MHC-I levels do not need to be maintained to evade NK-cell recognition. Tumors may downregulate MHC-I expression to avoid recognition by cytotoxic T cells, which remain intact and functional in NKC^{KD} mice. This MHC-I-low phenotype persists following transplantation into a WT environment, rendering tumors from NKC^{KD} animals susceptible to recognition and killing by NK cells with missing-self capability in WT mice.

Dadi and colleagues showed the presence of tissue-resident type-1–like innate lymphoid cells (ILC1l) and type 1 innate-like T cells (ILTC1) in mammary tumors from MMTV-PyVT mice (22).

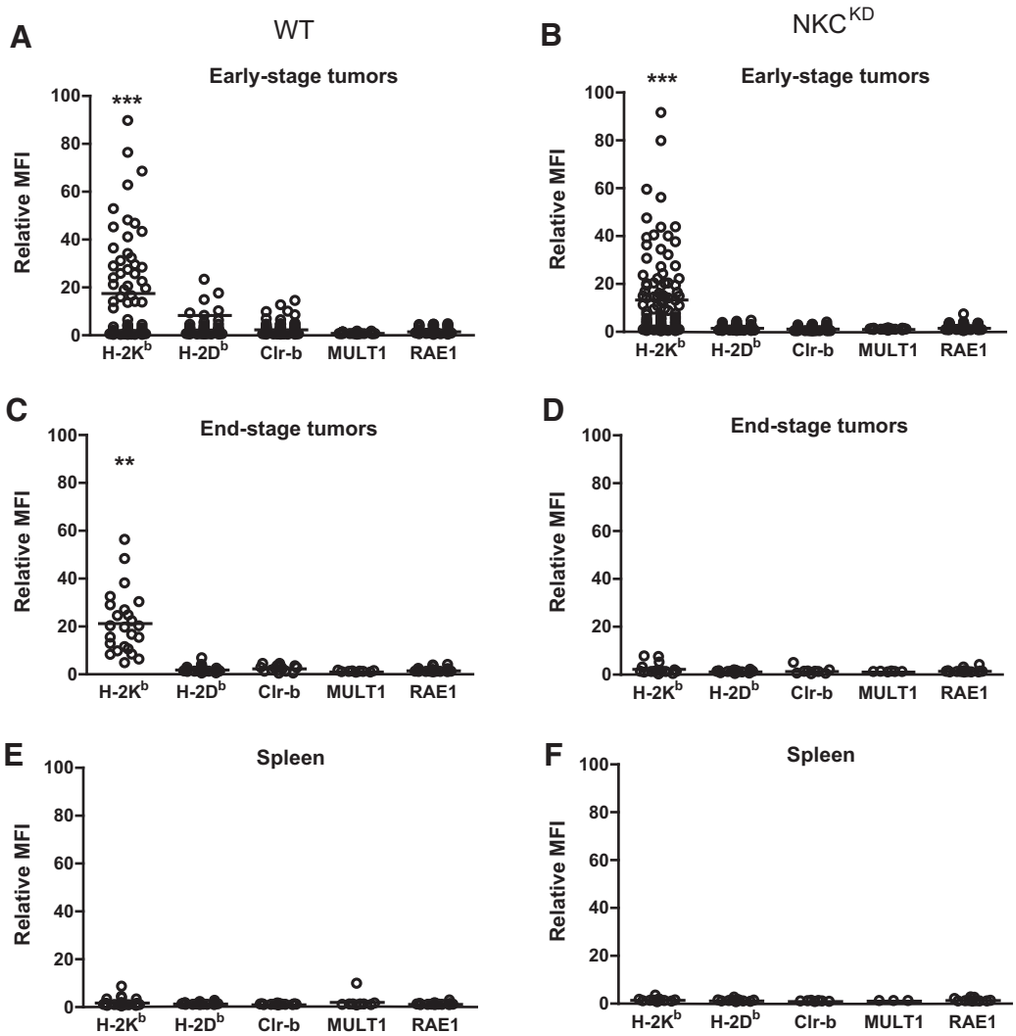

Figure 4.

Alterations in MHC-I expression on mammary tumors over time due to altered NK-cell receptor expression. **A** and **B,** *Ex vivo* analysis of early-stage mammary tumors from PyVT^{Tg} mice on WT ($n = 92$) and NKC^{KD} ($n = 101$) backgrounds. **C** and **D**, endpoint tumors from PyVT^{Tg} mice on WT ($n = 24$) and NKC^{KD} ($n = 26$) backgrounds. **E** and **F**, spleens from the same tumor-bearing WT ($n = 24$) and NKC^{KD} ($n = 26$) mice. *n* represents number of tumors analyzed. Surface expression was analyzed by antibody labelling and flow cytometry. For tumors, MFI was standardized to expression on mammary epithelial cells from fat pads of WT, non–MMTV-PyVT transgenic mice. For spleens, MFI was standardized to expression on total splenocytes from WT, non–MMTV-PyVT transgenic mice. Each dot represents a single tumor. Horizontal line represents mean.

These cells are characterized by high expression of NK1.1 antigen, a prototypic marker for NK cells in B6 mice; however, they are distinct from the conventional NK and NKT cells. These ILTC1 cells expand in early tumors, express granzyme B, and are able to kill tumor cells in *in vitro* assays, indicating a role in cancer immunosurveillance. As the B6.NKC^{KD} and B6.Ly49^{129} congenic mouse strains used in our study possess a 129-derived NKC (described in Materials and Methods), these mice do not express the NK1.1 antigen. Therefore, we are unable to rule out the contribution of ILC1l and ILTC1 cells in Ly49-mediated tumor immunosurveillance and immunoediting (22). Expression of the inhibitory Ly49C and Ly49I, the educating self–MHC-I–specific Ly49 receptors in B6 mice, has not been reported on these cells, and their contribution to ILC1l- and ILTC1-mediated cancer immunosurveillance remains to be determined. Although our study provides evidence for the role of MHC-I receptors expressed on NK cells in breast cancer immunosurveillance and immunoediting, further evaluation of receptor expression on innate immune cells, other than NK cells, will improve understanding of how different immune cells contribute to this phenomenon. Nevertheless, NK cells contribute to breast cancer control.

A retrospective study comparing the molecular tumor signatures of breast cancer patients with relapse or relapse-free survival found that the expression of NK-cell activating receptors NKp30 and NKp44 and adhesion molecule LFA-1 is correlated with favorable prognosis and a lack of cancer recurrence (36). In a separate study, patients with malignant disease had weaker NK cell-mediated lytic capabilities than those with benign tumors,

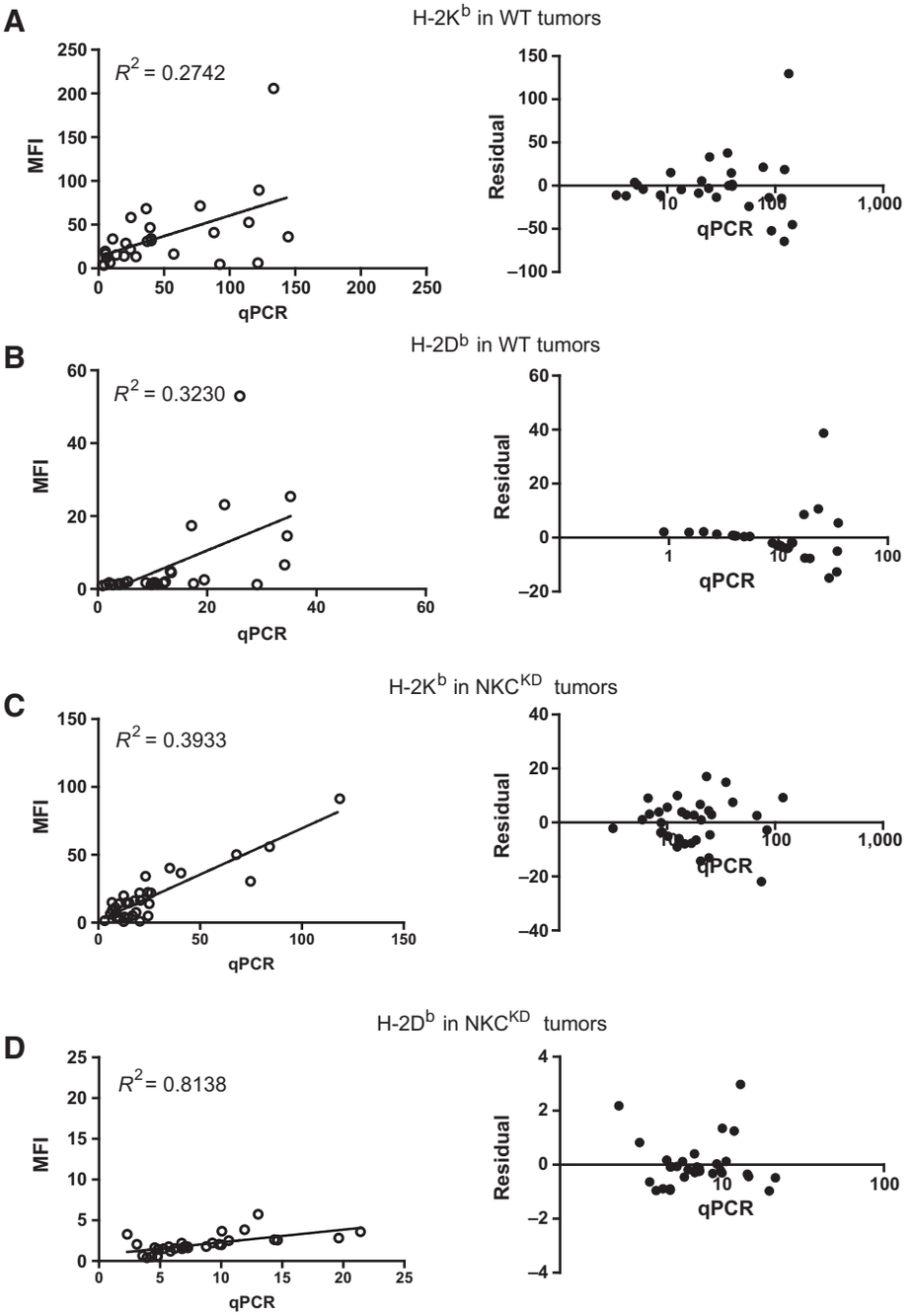

Figure 5.
Comparison of mammary tumor H-2K^b and H-2D^b expression using qPCR and flow cytometry. Analysis of tumors isolated from WT mice for (**A**) H-2K^b and (**B**) H-2D^b expression, and NKC^{KD} mice for **(C)** H-2K^b and (**D**) H-2D^b expression. Left, comparison of data acquired from qPCR compared with flow cytometry. Right, residual plots of the corresponding comparison. Each mouse represents an independent experiment. qPCR performed in triplicate.

and NK cells from patients with early disease (stage I) were more lytic than those from late-stage (II–IV) patients (37). Finally, advanced breast cancer patients had an increased proportion of immature and noncytotoxic NK-cell subsets in their peripheral blood (38).

Our study and others show that breast tumor cells express ligands for both activating and inhibitory NK-cell receptors (39). Similar to our finding of the importance of MHC-I expression on breast tumor cells, Mamessier and colleagues identified HLA receptors (KIRs and/or NKG2A) as important for NK recognition of breast tumor cells (39). Kaneko and colleagues show MHC-I upregulation in approximately 70% of their studied cases, similar to what we reported in our MMTV-PyVT–derived early-stage tumors (40). There is little or no expression of MHC-I in normal mammary tissue, therefore, positive staining of tumors for MHC-1 expression suggests MHC-I upregulation. The remaining 30%—in which no MHC-I upregulation was observed—could be due to the absence of KIR and HLA haplotypes, suggesting that these patients have uneducated NK cells like those in our NKC^{KD}

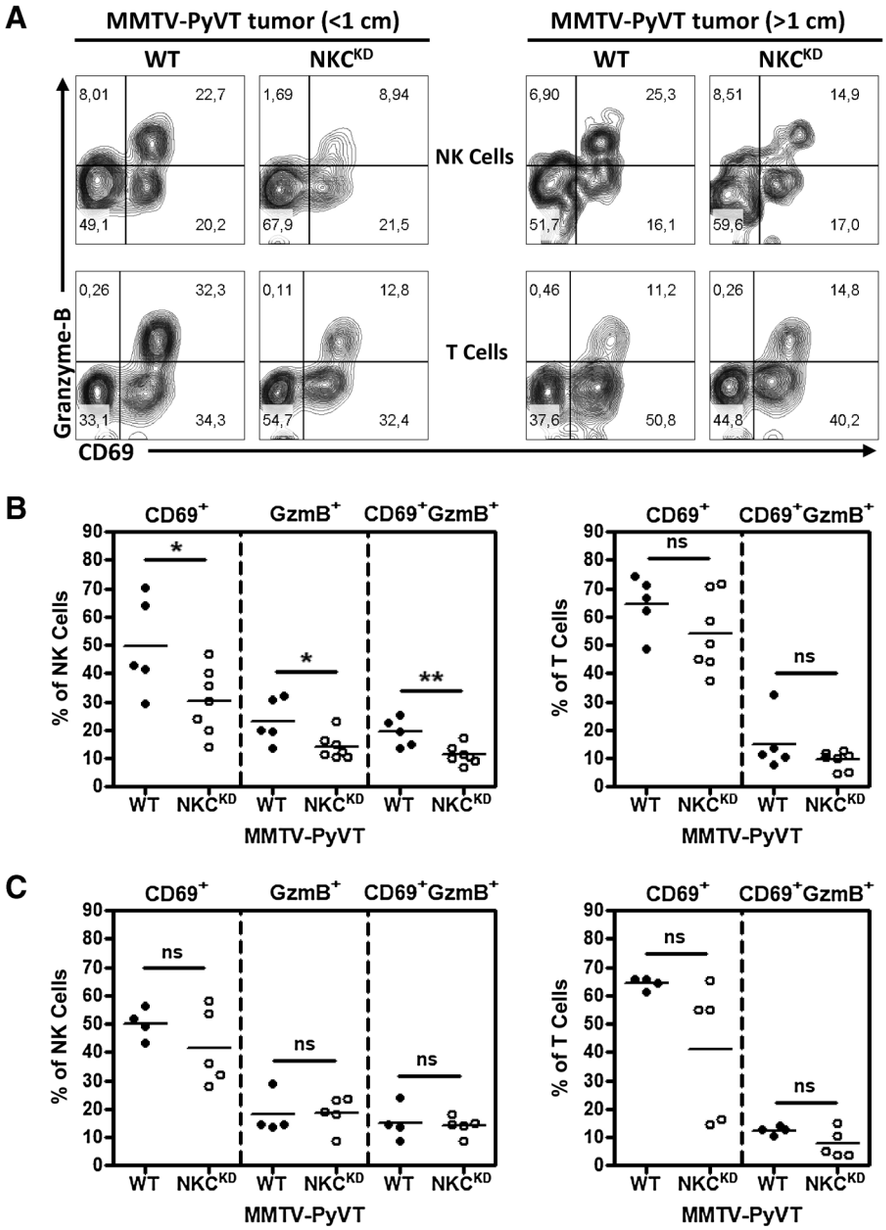

Figure 6.

Analysis of TILs in mammary tumors from MMTV-PyVT^{Tg} mice. **A,** Tumor-infiltrating NK cells (NKp46^{+}CD3^{-}) and T cells (NKp46^{-}CD3^{+}) in early (<1 cm) and end-stage tumors (>1 cm) from WT and NKC^{KD} mice were stained *ex vivo* for activation marker CD69 and granzyme B production, and analyzed by flow cytometry. Representative plots from one mouse are shown. Cell percentages are indicated in each quadrant. **B,** Frequency of activated tumor-infiltrating NK and T cells based on CD69 and granzyme B production in early-stage tumors. **C,** Frequency of activated tumor-infiltrating NK and T cells based on CD69 and granzyme B production in end-stage tumors. Each dot represents a single tumor. Horizontal line, mean value.

mice. Unfortunately, for the human data samples we do not know the HLA and KIR type of these patients.

Another study has also observed altered NK-cell function in a murine model of spontaneously developing invasive mammary tumors using the MMTV/Neu transgenic model, which is similar to the Py-VT transgenic model in our study (41). Mice deficient in the NK lytic-associated molecule were more susceptible to primary and metastatic tumor growth (42, 43). Although we observed primary tumor control defects in our NKC^{KD} mice, we saw no difference in the metastasis levels. Our analysis of gross pathology of the lung may not have been sensitive enough to detect a difference between our WT and NKC^{KD} group; GFP expression was used in the aforementioned study (43).

Further work into tumor-infiltrating NK cells could provide a better understanding of their functional capabilities in cancer patients. Tumor-infiltrating NK cells in human breast cancer possess an uneducated phenotype (38). As well, NK cells isolated from Py-VT transgenic mouse mammary tumors were CD27^{low}CD11b^{low}, suggestive of an immature phenotype, and exhibited decreased levels of DX5 (44). Given education is a plastic process (45, 46), the educated NK cells, upon tumor infiltration and exposure to the MHC-I–low tumor microenvironment, may themselves become uneducated. The latter may be a result of known low levels of MHC-I in late-stage tumors (47). Thus, NKC^{KD} mice might serve as a model for established late-stage breast cancer as most NK cells in these mice are Ly49 uneducated.

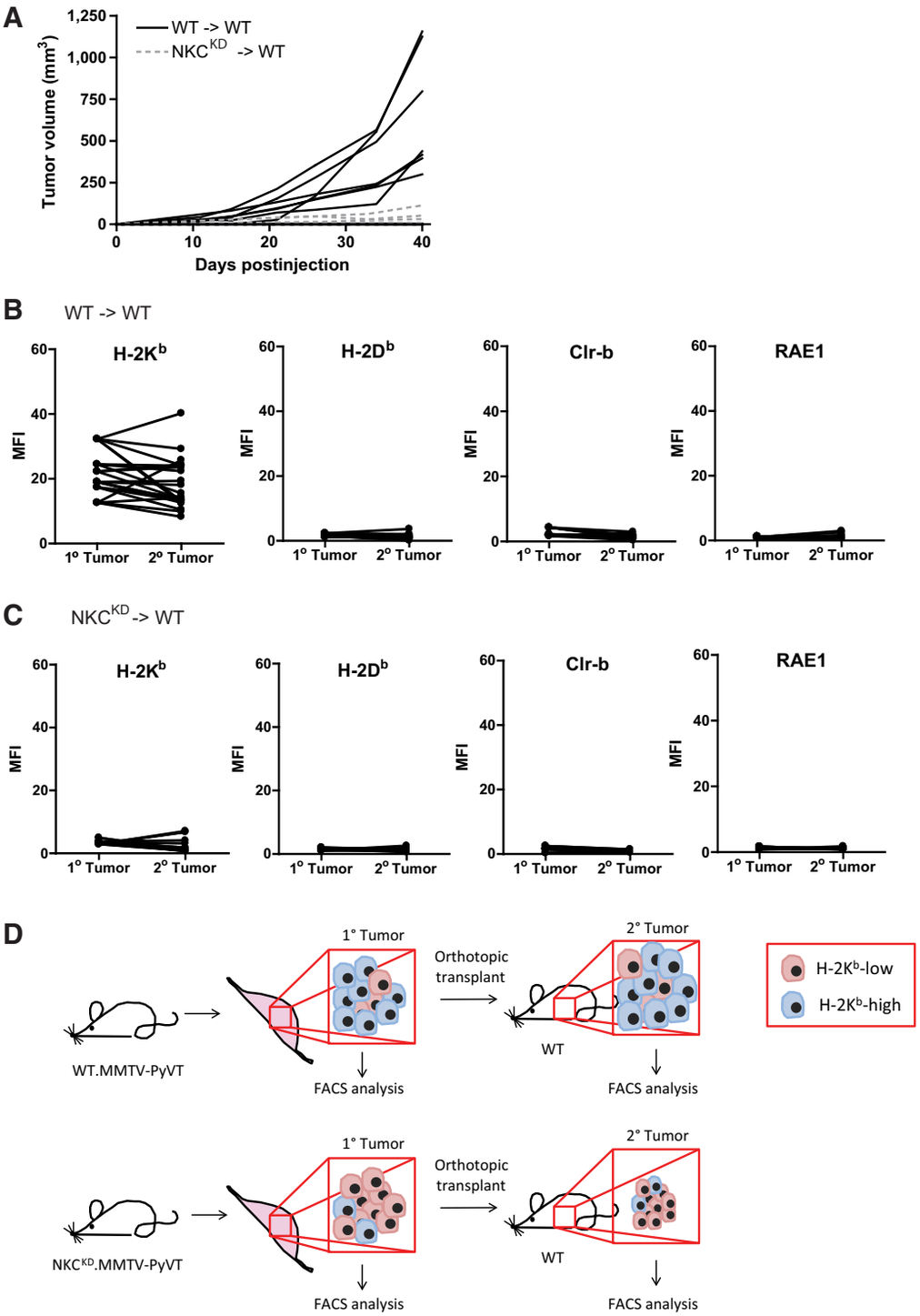

Figure 7.

Altered MHC-I expression of primary tumors affects tumorigenicity in naïve WT recipients. Tumor cells from MMTV-PyVT mice on WT and NKC^{KD} backgrounds were injected into the mammary fat pads of groups of naïve WT mice. **A,** Tumor growth curves following transplantation of primary tumor into secondary WT recipient. Each line represents a single mouse. **B,** Expression levels of H-2K^{b}, H-2D^{b}, Clr-b, and Rae1 in WT-derived primary tumor (1° Tumor) and transplanted tumors following growth in recipient WT mice (2° Tumor; $n = 23$). **C,** Expression levels of H-2K^{b}, H-2D^{b}, Clr-b, and Rae1 in NKC^{KD}-derived primary tumor (1° Tumor) and transplanted tumors following growth in recipient WT mice (2° Tumor; $n = 15$). **D,** Schematic model of WT- or NKC^{KD}-derived primary tumor transplantation into WT naïve recipient mice.

Similar to our tumor evasion results, work by Mamessier and colleagues suggests that breast tumor cells secrete soluble inhibitory factors that alter NK-cell function (39). Liu and colleagues have also shown that murine mammary tumor-derived exosomes can inhibit NK cells (48). In the presence of these secreted tumor exosomes, NK-cell proliferation and cytotoxicity are reduced and tumor growth increases (48). Similarly, tumor cells secrete soluble ligands for the activating receptor NKG2D that dampen NK-cell responses (49). Although we saw no differences in surface NKG2D ligands (Fig. 4), we cannot rule out the presence of these soluble ligands.

The heterogeneity and plasticity of immune cell subsets, which appears to be dependent on the microenvironment, could be an advantage in patient treatments because these cells would be amenable to modulation. The NK cell's response to an encounter with another cell is dependent on a balance of activating and inhibitory receptors. A better understanding of the role of these receptors in cancer detection and elimination will help with design of future NK cell–based therapies. In this study, we show MHC-I–directed immunoediting in a solid cancer in the absence of Ly49 receptors, as seen in NKC^{KD} mice. NK cells and Ly49 receptors play a critical role in breast cancer immunosurveillance. A better understanding of the HLA and KIR haplotype correlation in breast cancer patients could provide better targeted treatment. NK cell–based treatments, instead of or in addition to T cell–based treatments of patients with MHC-I-low tumors, could deliver greater clinical successes.

Disclosure of Potential Conflicts of Interest

No potential conflicts of interest were disclosed.

Authors' Contributions

Conception and design: M.M. Tu, M.M.A. Rahim, A.P. Makrigiannis
Development of methodology: M.M. Tu, A.B. Mahmoud
Acquisition of data (provided animals, acquired and managed patients, provided facilities, etc.): M.M. Tu, M.M.A. Rahim, C. Sayed, A.B. Mahmoud
Analysis and interpretation of data (e.g., statistical analysis, biostatistics, computational analysis): M.M. Tu, M.M.A. Rahim, C. Sayed
Writing, review, and/or revision of the manuscript: M.M. Tu, M.M.A. Rahim, A.P. Makrigiannis
Administrative, technical, or material support (i.e., reporting or organizing data, constructing databases): A.P. Makrigiannis
Study supervision: A.P. Makrigiannis

Acknowledgments

The authors would like to thank Rashida Rajgara for assistance with qPCR.

Grant Support

This work was supported by Innovation (#702450) and Innovation to Impact (#703935-1) grants from the Canadian Cancer Society Research Institute, and an Establishment grant from Nova Scotia Health Research Foundation to A.P. Makrigiannis. M.M. Tu was supported by an Ontario Graduate Scholarship.

The costs of publication of this article were defrayed in part by the payment of page charges. This article must therefore be hereby marked *advertisement* in accordance with 18 U.S.C. Section 1734 solely to indicate this fact.

Received January 31, 2017; revised July 17, 2017; accepted September 8, 2017; published OnlineFirst September 18, 2017.

References

1. Bray F, McCarron P, Parkin DM. The changing global patterns of female breast cancer incidence and mortality. Breast Cancer Res BCR 2004;6:229–39.
2. Al-Hajj M, Wicha MS, Benito-Hernandez A, Morrison SJ, Clarke MF. Prospective identification of tumorigenic breast cancer cells. Proc Natl Acad Sci USA 2003;100:3983–8.
3. Bao S, Wu Q, McLendon RE, Hao Y, Shi Q, Hjelmeland AB, et al. Glioma stem cells promote radioresistance by preferential activation of the DNA damage response. Nature 2006;444:756–60.
4. Hambardzumyan D, Squatrito M, Squartro M, Holland EC. Radiation resistance and stem-like cells in brain tumors. Cancer Cell 2006;10:454–6.
5. Woodward WA, Chen MS, Behbod F, Alfaro MP, Buchholz TA, Rosen JM. WNT/beta-catenin mediates radiation resistance of mouse mammary progenitor cells. Proc Natl Acad Sci USA 2007;104:618–23.
6. Dunn GP, Old LJ, Schreiber RD. The three Es of cancer immunoediting. Annu Rev Immunol 2004;22:329–60.
7. Fridman WH, Pagès F, Sautès-Fridman C, Galon J. The immune contexture in human tumours: impact on clinical outcome. Nat Rev Cancer 2012;12:298–306.
8. Kaplan DH, Shankaran V, Dighe AS, Stockert E, Aguet M, Old LJ, et al. Demonstration of an interferon gamma-dependent tumor surveillance system in immunocompetent mice. Proc Natl Acad Sci USA 1998;95:7556–61.
9. Shankaran V, Ikeda H, Bruce AT, White JM, Swanson PE, Old LJ, et al. IFNgamma and lymphocytes prevent primary tumour development and shape tumour immunogenicity. Nature 2001;410:1107–11.
10. Imai K, Matsuyama S, Miyake S, Suga K, Nakachi K. Natural cytotoxic activity of peripheral-blood lymphocytes and cancer incidence: an 11-year follow-up study of a general population. Lancet Lond Engl 2000;356:1795–9.
11. Coca S, Perez-Piqueras J, Martinez D, Colmenarejo A, Saez MA, Vallejo C, et al. The prognostic significance of intratumoral natural killer cells in patients with colorectal carcinoma. Cancer 1997;79:2320–8.
12. Ishigami S, Natsugoe S, Tokuda K, Nakajo A, Che X, Iwashige H, et al. Prognostic value of intratumoral natural killer cells in gastric carcinoma. Cancer 2000;88:577–83.
13. Villegas FR, Coca S, Villarrubia VG, Jiménez R, Chillón MJ, Jareño J, et al. Prognostic significance of tumor infiltrating natural killer cells subset CD57 in patients with squamous cell lung cancer. Lung Cancer Amst Neth 2002;35:23–8.
14. Albertsson PA, Basse PH, Hokland M, Goldfarb RH, Nagelkerke JF, Nannmark U, et al. NK cells and the tumour microenvironment: implications for NK-cell function and anti-tumour activity. Trends Immunol 2003;24:603–9.
15. Esendagli G, Bruderek K, Goldmann T, Busche A, Branscheid D, Vollmer E, et al. Malignant and non-malignant lung tissue areas are differentially populated by natural killer cells and regulatory T cells in non-small cell lung cancer. Lung Cancer Amst Neth 2008;59:32–40.
16. Kärre K, Ljunggren HG, Piontek G, Kiessling R. Selective rejection of H-2-deficient lymphoma variants suggests alternative immune defence strategy. Nature 1986;319:675–8.
17. Raulet DH, Vance RE. Self-tolerance of natural killer cells. Nat Rev Immunol 2006;6:520–31.
18. Tu MM, Mahmoud AB, Wight A, Mottashed A, Bélanger S, Rahim MMA, et al. Ly49 family receptors are required for cancer immunosurveillance mediated by natural killer cells. Cancer Res 2014;74:3684–94.
19. Bélanger S, Tu MM, Rahim MMA, Mahmoud AB, Patel R, Tai L-H, et al. Impaired natural killer cell self-education and "missing-self" responses in Ly49-deficient mice. Blood 2012;120:592–602.
20. O'Sullivan T, Saddawi-Konefka R, Vermi W, Koebel CM, Arthur C, White JM, et al. Cancer immunoediting by the innate immune system in the absence of adaptive immunity. J Exp Med 2012;209:1869–82.
21. Smyth MJ, Crowe NY, Godfrey DI. NK cells and NKT cells collaborate in host protection from methylcholanthrene-induced fibrosarcoma. Int Immunol 2001;13:459–63.

22. Dadi S, Chhangawala S, Whitlock BM, Franklin RA, Luo CT, Oh SA, et al. Cancer immunosurveillance by tissue-resident innate lymphoid cells and innate-like T cells. Cell 2016;164:365–77.
23. Tirona MT, Sehgal R, Ballester O. Prevention of breast cancer (part I): epidemiology, risk factors, and risk assessment tools. Cancer Invest 2010; 28:743–50.
24. Sørlie T, Wang Y, Xiao C, Johnsen H, Naume B, Samaha RR, et al. Distinct molecular mechanisms underlying clinically relevant subtypes of breast cancer: gene expression analyses across three different platforms. BMC Genomics 2006;7:127.
25. Guy CT, Cardiff RD, Muller WJ. Induction of mammary tumors by expression of polyomavirus middle T oncogene: a transgenic mouse model for metastatic disease. Mol Cell Biol 1992;12:954–61.
26. Patel R, Bélanger S, Tai L-H, Troke AD, Makrigiannis AP. Effect of Ly49 Haplotype Variance on NK Cell Function and Education. J Immunol 2010;185:4783–92.
27. Ran FA, Hsu PD, Wright J, Agarwala V, Scott DA, Zhang F. Genome engineering using the CRISPR-Cas9 system. Nat Protoc 2013;8:2281–308.
28. Belanger S, Tai L-H, Anderson SK, Makrigiannis AP. Ly49 cluster sequence analysis in a mouse model of diabetes: an expanded repertoire of activating receptors in the NOD genome. Genes Immun 2008;9:509–21.
29. Schefe JH, Lehmann KE, Buschmann IR, Unger T, Funke-Kaiser H. Quantitative real-time RT-PCR data analysis: current concepts and the novel "gene expression's CT difference" formula. J Mol Med Berl Ger 2006; 84:901–10.
30. Kiessling R, Klein E, Pross H, Wigzell H. "Natural" killer cells in the mouse. II. Cytotoxic cells with specificity for mouse Moloney leukemia cells. Characteristics of the killer cell. Eur J Immunol 1975;5:117–21.
31. Ewens A, Mihich E, Ehrke MJ. Distant metastasis from subcutaneously grown E0771 medullary breast adenocarcinoma. Anticancer Res 2005;25: 3905–15.
32. Sirotnak FM, DeGraw JI, Schmid FA, Goutas LJ, Moccio DM. New folate analogs of the 10-deaza-aminopterin series. Further evidence for markedly increased antitumor efficacy compared with methotrexate in ascitic and solid murine tumor models. Cancer Chemother Pharmacol 1984;12:26–30.
33. Zhou F.Molecular mechanisms of IFN-gamma to up-regulate MHC class I antigen processing and presentation. Int Rev Immunol 2009;28:239–60.
34. Takeda K, Nakayama M, Hayakawa Y, Kojima Y, Ikeda H, Imai N, et al. IFN-γ is required for cytotoxic T cell-dependent cancer genome immunoediting. Nat Commun 2017;8:14607.
35. Caras I, Grigorescu A, Stavaru C, Radu DL, Mogos I, Szegli G, et al. Evidence for immune defects in breast and lung cancer patients. Cancer Immunol Immunother CII 2004;53:1146–52.
36. Ascierto ML, Idowu MO, Zhao Y, Khalak H, Payne KK, Wang X-Y, et al. Molecular signatures mostly associated with NK cells are predictive of relapse free survival in breast cancer patients. J Transl Med 2013; 11:145.
37. Garner WL, Minton JP, James AG, Hoffmann CC. Human breast cancer and impaired NK cell function. J Surg Oncol 1983;24:64–6.
38. Mamessier E, Pradel LC, Thibult M-L, Drevet C, Zouine A, Jacquemier J, et al. Peripheral blood NK cells from breast cancer patients are tumor-induced composite subsets. J Immunol Baltim Md 1950 2013;190: 2424–36.
39. Mamessier E, Sylvain A, Bertucci F, Castellano R, Finetti P, Houvenaeghel G, et al. Human breast tumor cells induce self-tolerance mechanisms to avoid NKG2D-mediated and DNAM-mediated NK cell recognition. Cancer Res 2011;71:6621–32.
40. Kaneko K, Ishigami S, Kijima Y, Funasako Y, Hirata M, Okumura H, et al. Clinical implication of HLA class I expression in breast cancer. BMC Cancer 2011;11:454.
41. Mamessier E, Sylvain A, Thibult M-L, Houvenaeghel G, Jacquemier J, Castellano R, et al. Human breast cancer cells enhance self tolerance by promoting evasion from NK cell antitumor immunity. J Clin Invest 2011;121:3609–22.
42. Hoover RG, Gullickson G, Kornbluth J. Impaired NK cytolytic activity and enhanced tumor growth in NK lytic-associated molecule-deficient mice. J Immunol Baltim Md 1950 2009;183:6913–21.
43. Hoover RG, Gullickson G, Kornbluth J. Natural killer lytic-associated molecule plays a role in controlling tumor dissemination and metastasis. Front Immunol 2012;3:393.
44. Krneta T, Gillgrass A, Chew M, Ashkar AA. The breast tumor microenvironment alters the phenotype and function of natural killer cells. Cell Mol Immunol 2016;13:628–39.
45. Elliott JM, Wahle JA, Yokoyama WM. MHC class I-deficient natural killer cells acquire a licensed phenotype after transfer into an MHC class I-sufficient environment. J Exp Med 2010;207:2073–9.
46. Joncker NT, Shifrin N, Delebecque F, Raulet DH. Mature natural killer cells reset their responsiveness when exposed to an altered MHC environment. J Exp Med 2010;207:2065–72.
47. Goepel JR, Rees RC, Rogers K, Stoddard CJ, Thomas WE, Shepherd L. Loss of monomorphic and polymorphic HLA antigens in metastatic breast and colon carcinoma. Br J Cancer 1991;64:880–3.
48. Liu C, Yu S, Zinn K, Wang J, Zhang L, Jia Y, et al. Murine mammary carcinoma exosomes promote tumor growth by suppression of NK cell function. J Immunol Baltim Md 1950 2006;176:1375–85.
49. Groh V, Wu J, Yee C, Spies T. Tumour-derived soluble MIC ligands impair expression of NKG2D and T-cell activation. Nature 2002;419:734–8.